Gümüşhane University Journal of Science and Technology

GUFBD / *GUJS* (2016) 16(3): 850-866 doi: 10.17714/gumusfenbil.1879397 Research Article

In-silico investigation of structural, electronic and biological properties of 2-[5-(4-chlorophenyl)-1*H*-pyrazole-3-yl]-6-(2-hydroxymethyl-1-methylpyrrolidine-3-yl)-3,5-dimethoxy-phenol compound

Ercan AVİNÇ[1], Kenan GÖREN[1]*, Ümit YILDIKO[2]

[1]*Kafkas University, Faculty of Science and Arts, Department of Chemistry, 36000, Kars, Turkey*

[2]*Kafkas University, Architecture and Engineering Faculty, Department of Bioengeering, 36000, Kars, Turkey*

• Received: 01.02.2026 • Accepted: 12.08.2026

Abstract

Pyrazole derivatives occupy an important position in medicinal and pharmaceutical research owing to their diverse biological properties. Among these activities, anti-inflammatory and analgesic effects have attracted considerable attention because pyrazole-based compounds are known to interact with important mediators involved in inflammatory pain pathways. However, studies systematically investigating the relationship between molecular structure and the physicochemical/electronic properties of these compounds remain limited. In the present study, the structural, electronic, and biological properties of 2-[5-(4-chlorophenyl)-1H-pyrazole-3-yl]-6-(2-hydroxymethyl-1-methylpyrrolidine-3-yl)-3,5-dimethoxyphenol (HMP2) were comprehensively examined using in silico approaches. The most stable molecular geometry was optimized at the second-order Møller–Plesset perturbation theory (MP2) level, and structural stability was evaluated through bond lengths and bond angles. Chemical reactivity and kinetic stability were assessed using HOMO–LUMO energy gap calculations, while electrophilic and nucleophilic regions were identified through molecular electrostatic potential (MEP) maps. Intramolecular charge-transfer behavior was investigated using nonlinear optical (NLO) properties, Mulliken atomic charge distributions, and Natural Bond Orbital (NBO) analyses. Furthermore, molecular docking studies against inflammation-related target proteins revealed that HMP2 exhibits favorable binding modes and strong binding affinities, indicating its potential anti-inflammatory activity. ADMET predictions further demonstrated that the compound possesses acceptable pharmacokinetic and toxicological characteristics. These findings suggest that HMP2 may be considered a promising candidate for the development of novel anti-inflammatory agents**.**

Keywords: Electronic structure, Inflammatory pain, In silico analysis, Molecular docking, Pyrazole derivatives

1. Introduction

Pyrazoles and their derivatives belong to an important class of nitrogen-containing heterocyclic compounds and are widely recognized as privileged scaffolds in medicinal chemistry. These compounds exhibit a broad spectrum of biological activities, including antimicrobial, antiviral, antitumor, analgesic, and anti-inflammatory effects (Sharma et al., 2026). Particularly, pyrazole-based derivatives have gained remarkable interest as potential anti-inflammatory agents because several clinically relevant pyrazole-containing drugs exert their pharmacological effects through the modulation of cyclooxygenase enzymes and inflammatory mediators (Anwer et al., 2026; Ram et al., 2026). Therefore, understanding the structural modification of pyrazole derivatives and their interactions with biological targets is of great importance for the development of new therapeutic agents.

At present, quantum chemical calculations are extensively employed in molecular design processes because they enable rapid and cost-effective evaluation of structural and electronic properties compared with experimental approaches. Computational techniques such as molecular geometry optimization, total energy calculations, HOMO–LUMO analysis, and molecular electrostatic potential (MEP) mapping provide valuable insight into molecular reactivity, stability, and charge distribution (Gören & Yıldıko, 2024). Among these methods, second-order Møller–Plesset perturbation theory (MP2) is frequently preferred for geometry and energy calculations of organic molecules because it accounts for electron correlation effects with higher

*Kenan GÖREN; kenangoren49@gmail.com

accuracy (Cremer, 2011). The HOMO–LUMO energy gap is regarded as an important descriptor of molecular reactivity and kinetic stability. A smaller energy gap generally indicates higher electron-transfer capability and enhanced chemical reactivity, whereas a larger gap suggests greater molecular stability (Bağlan, Gören, et al., 2023b). Likewise, MEP maps are useful for identifying electrophilic and nucleophilic regions, thereby facilitating the interpretation of intermolecular interactions with biological macromolecules (Cherian & Ravikumar, 2026).

Inflammatory pain is a complex pathological condition mediated by increased prostaglandin synthesis, cytokine release, oxidative stress, and neuronal sensitization. Proteins such as cyclooxygenase-2 (COX-2), tumor necrosis factor-alpha (TNF-α), and interleukin-1 beta (IL-1β) play central roles in these pathways and are considered important molecular targets for anti-inflammatory drug discovery (Aysha et al., 2026; Kotia et al., 2026). In modern drug development, molecular docking has become an indispensable tool for predicting ligand–protein interactions. Docking studies provide valuable information regarding binding affinity, binding orientation, and interaction types within the active site of target proteins (Agbektas et al., 2026). Accordingly, evaluating pyrazole derivatives against inflammation-associated proteins may provide useful insights into their therapeutic potential. However, binding affinity alone is insufficient to evaluate the therapeutic potential of a compound. The ADMET profile Absorption, Distribution, Metabolism, Excretion, and Toxicity is a critical determinant of clinical success. In silico ADMET prediction enables early-stage assessment of pharmacokinetic behavior and toxicological risks, thereby reducing the cost and time associated with drug development (Bağlan et al., 2026; Çimen et al., 2026). Consequently, ADMET evaluation has become a standard step in the screening of newly designed or synthesized molecules.

This study is based on the hypothesis that the synthesized HMP2 compound may exhibit significant anti-inflammatory potential through effective interaction with key inflammatory target enzymes, particularly cyclooxygenase-2 (COX-2), supported by favorable structural stability and electronic properties. It is further hypothesized that the electronic distribution and molecular geometry of HMP2 may contribute to its binding affinity and reactivity profile, thereby influencing its pharmacological behavior. To test this hypothesis, a comprehensive computational strategy was employed. Density Functional Theory (DFT) calculations were performed to evaluate structural optimization and electronic stability. HOMO–LUMO analysis was used to investigate chemical reactivity and kinetic stability. Molecular Electrostatic Potential (MEP) and Mulliken charge analyses were conducted to identify electrophilic and nucleophilic regions relevant for biological interactions. Natural Bond Orbital (NBO) analysis was applied to understand intramolecular charge delocalization and stabilization effects. In addition, nonlinear optical (NLO) properties were examined to assess optoelectronic behavior. Molecular docking studies were carried out to predict binding affinity toward COX-2 (PDB: 6COX) and related inflammatory targets, while ADMET analysis was performed to evaluate pharmacokinetic and drug-likeness properties.

2. Materials and methods

The initial structure of the HMP2 molecule was drawn using ChemDraw 20.0 and obtained in.mol format. Subsequently, geometric optimization operations were performed using Gaussian 09 software (Trucks et al., 2009). The most stable conformer of the molecule was determined, and the optimization process was carried out at the second order (MP2) level of the Møller–Plesset perturbation theory, using the 6-31G(d,p) and LANL2DZ basis sets. Molecular docking studies were performed using the AutoDock Vina program (Eberhardt et al., 2021) to evaluate the ability of HMP2 to bind to target proteins associated with inflammatory pain. Proteins such as PDB:3LN1 (Bank, 2013) and PDB:6COX (Bank, 2017), which play critical roles in inflammation and pain pathways, were selected as protein targets. The crystal structures of the target proteins were downloaded from the Protein Data Bank (PDB) database in .pdb format. Binding modes and interactions were visualized and analyzed using Discovery Studio Visualizer programs (BIOVIA, 2016). ADMET (Pharmacokinetic and toxicological) predictions: The pharmacokinetic and toxicological profile of the HMP2 compound was determined using the AdmetLab 2.0 program (ADMETlab 2.0, n.d.)

3. Results and discussion

3.1. Structure details and analysis

Molecular geometry describes the arrangement of atoms in a molecule in three-dimensional space and is a fundamental element determining the physical and chemical properties of the molecule (Bağlan et al.,

2023a). Conformation refers to the different spatial arrangements resulting from rotations around bonds, and these changes have significant effects on the molecule's energy level, stability, chemical reactivity, and biological activity (Bağlan et al., 2022). The theoretical calculation results presented in Table 1 and Table 2 reveal that the geometric parameters of the HMP2 molecule show slight differences depending on the calculation method used. While the bond lengths obtained with the 6-311G(d,p) and LANL2DZ basis sets are generally consistent, the LANL2DZ method yielded longer values, particularly in C–C and C–N bonds. This difference can be attributed to the LANL2DZ basis set containing an effective nuclear potential and being less flexible. In C–O bonds, the 6-311G(d,p) method yielded shorter bond lengths. Only minor differences were observed between the two methods for C–H and O–H bonds, with the LANL2DZ method predicting O–H bonds to be relatively longer. When bond angles were examined, both methods showed an approximately trigonal planar structure in aromatic and heterocyclic regions. However, significant differences existed between the methods in some bond angles, particularly in regions containing heteroatoms. Bond angles C5–C9–C10, C3–C38–C40, and C1–C6–O7 showed sensitivity to the calculation method. The dihedral angles given in Table 2 show that the HMP2 molecule has a largely planar conformation with both methods. The fact that most dihedral angles are around ±180° reveals that the molecule's rings and functional groups are located in almost the same plane; the sign differences between the methods are solely due to spatial orientation reversal. In conclusion, both calculation methods confirm that the HMP2 molecule has a stable and largely planar structure. However, the 6-311G(d,p) basis set provides more reliable results in defining the molecular geometry by more precisely defining bond lengths and bond angles. The consistency of the obtained geometric parameters with data from DFT and X-ray crystallography studies on similar compounds containing pyrazole cores supports the reliability of the calculation results (Karruchi et al., 2017; Deshmukh et al., 2025). The geometric structure of the HMP2 compound optimized using the LANL2DZ basis set has been presented in Figure 1.

Table 1. Theoretically determined bond lengths (Å) of the HMP2 molecule

Bond Lengths	6-311G(d,p)	LANL2DZ	Bond Lengths	6-311G(d,p)	LANL2DZ
C1-C2	1.40581	1.42569	C17-Cl22	1.73595	1.90034
C2-C3	1.41928	1.42796	C3-C38	1.51164	1.54399
C3-C4	1.41830	1.42794	C38-C39	1.68470	1.58588
C4-C5	1.40564	1.43078	C39-C42	1.54448	1.56072
C5-C6	1.42317	1.43723	C42-O43	1.43204	1.42377
C6-O7	1.35670	1.42508	C39-N45	1.40032	1.35090
O7-C8	1.41396	1.46149	N45-C46	1.43573	1.50158
C2-O22	1.38152	1.42377	N45-C41	1.43198	1.52229
O22-C45	1.42341	1.46526	C38-C40	1.71672	1.59426
C5-C9	1.48112	1.51132	C40-C41	1.50073	1.56072
C9-C10	1.43608	1.43486	C40-H50	1.08864	1.09750
C10-C11	1.37728	1.41103	C16-H30	1.08528	1.09515
C11-N12	1.39709	1.40944	N12-H28	1.01855	1.01749
N12-N13	1.38460	1.41697	C8-H25	1.09626	1.10233
C11-C14	1.46344	1.50037	O20- H33	0.96085	1.09292
C14-C15	1.41141	1.42996	C34- H35	1.09130	1.10691
C15-C16	1.39626	1.41421	O43-H44	0.96058	1.09210
C16-C25	1.40133	1.41553	C10- H27	1.08014	1.10742

Table 2. Theoretically determined bond angles (°) of the HMP2 molecule

Bond Angles	6-311G(d,p)	LANL2DZ	Bond Angles	6-311G(d,p)	LANL2DZ
C1–C6-O7	119.90842	125.62896	C3-C4-O20	113.13512	116.26884
C6-O7-C8	117.26023	112.62905	C5-C4-O20	120.45273	122.39495
C1-C2-O21	125.45527	125.42150	C3-C38-C40	103.42328	111.49881
C2-O21-C34	126.06512	112.59420	C38-C39-C42	130.24917	129.33482
C5-C9-N13	124.21300	120.21467	C38-C39-N45	120.08332	121.28887
C5-C9-C10	106.51616	127.90012	C38-C40-C41	101.74785	103.89138
N12-C11-C14	121.77048	123.50036	C39-C42-O43	125.32379	124.65131

Table 2. (Continued)

Planar Bond Angles	6-311G(d,p)	LANL2DZ	Planar Bond Angles	6-311G(d,p)	LANL2DZ
C5-C6-O7-C8	152.90652	-151.69661	C40-C41-N45-C46	177.20712	-176.37589
C2-C3-O9-C48	-173.13860	174.73713	C5-C9-N13-N12	179.08571	-178.56948
C11-C14-C19	121.04954	121.80461	C3-C2-O21	114.91162	113.90745
C18-C17-Cl22	119.85904	118.44977	N13-N12-C11	110.23872	109.26219
C4-C3-C2-O21	171.99663	-173.99779	C17-C18-N19-C21	-179.94683	-178.93682
C6-C5-C4-O11	178.88353	178.95165	C10-C11-C14-C19	-174.18202	-176.18101
C1-C6-C5-C9	173.54370	174.95264	C19-C18-C17-Cl22	-179.77420	-177.77328
C3-C38-C40-C41	-169.34607	170.10367	C15-C16-C17-Cl22	179.88082	179.77092

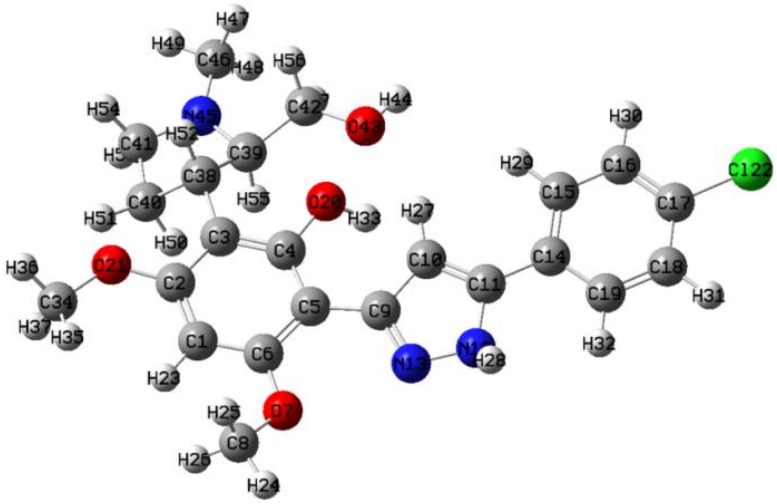

Figure 1. Optimized geometric representation of HMP2 compound with basis set LANL2DZ

3.2. HOMO and LUMO analysis

The highest occupied molecular orbital (HOMO) and the lowest unoccupied molecular orbital (LUMO) are called frontier molecular orbitals (FMOs) and play a significant role in determining the optical and electrical properties, chemical reactivity, and kinetic stability of molecules. The HOMO–LUMO energy gap is associated with σ→σ* and π→π* type electronic transitions according to molecular orbital theory and is a fundamental indicator of molecular reactivity (Bağlan et al., 2023). Molecules with a small energy gap exhibit high reactivity and low stability and are defined as "soft" molecules (Gören et al., 2024a). The frontier molecular orbitals of the HMP2 molecule were calculated using the 6-311G(d,p) and LANL2DZ basis sets. The results have been presented in Figures 2 and 3, respectively, and comparative HOMO–LUMO-based quantum chemical parameters are given in Table 3. The HOMO–LUMO energy gap (ΔE=4.7481 eV) calculated with the 6-311G(d,p) base set is larger compared to the LANL2DZ base set (ΔE=3.7365 eV), indicating that the molecule is more stable and less reactive. In contrast, the LANL2DZ base set, with its smaller energy gap, reveals a more reactive structure. The higher ionization potential (I) value for the 6-311G(d,p) base set indicates that electron removal is more difficult and the structure is more stable. The higher calculated electron affinity (A) for the LANL2DZ base set shows an increased tendency of the molecule to accept electrons. The chemical hardness (η) and softness (s) parameters also support these results, with the 6-311G(d,p) base set describing a harder and less polarizable structure, while the LANL2DZ base set describes the molecule as softer and more reactive. Chemical potential (μ) and electronegativity (χ) values were found to be similar for both base sets, but a more negative μ value was obtained with the 6-311G(d,p) base set. The electrophilicity index (ω) is higher for the LANL2DZ base set, indicating that the molecule exhibits a more dominant electrophilic character in this approach. Overall, the 6-311G(d,p) base set describes the HMP2 molecule as more stable and less reactive, while the LANL2DZ base set describes it as softer, more reactive, and more electrophilic.

Table 3. HOMO and LUMO quantum chemical properties calculated for the HMP2 molecule with 6-311G(d,p) and LANL2DZ principal settlers

Molecules Energy		6-311G(d,p)	LANL2DZ
E_{LUMO}		-2.0176	-2.3013
E_{HOMO}		-6.7657	-6.0378
E_{HOMO-1}		-6.8649	-6.7689
E_{LUMO+1}		-3.0190	-3.2876
Energy Gap	$(\Delta E)\lvert E_{HOMO}-E_{LUMO}\rvert$	4.7481	3.7365
Ionization Potential	$(I=-E_{HOMO})$	6.7657	6.0378
Electron Affinity	$(A=-E_{LUMO})$	2.0176	2.3013
Chemical hardness	$(\eta=(I-A)/2)$	2.3740	3.7365
Chemical softness	$(s=1/2\eta)$	1.1870	1.8680
Chemical Potential	$(\mu=-(I+A)/2)$	-4.3916	-4.1695
Electronegativity	$(\chi=(1+A)/2)$	1.5088	1.6506
Electrophilicity index	$(\omega=\mu 2/2\eta)$	4.0619	2.3263

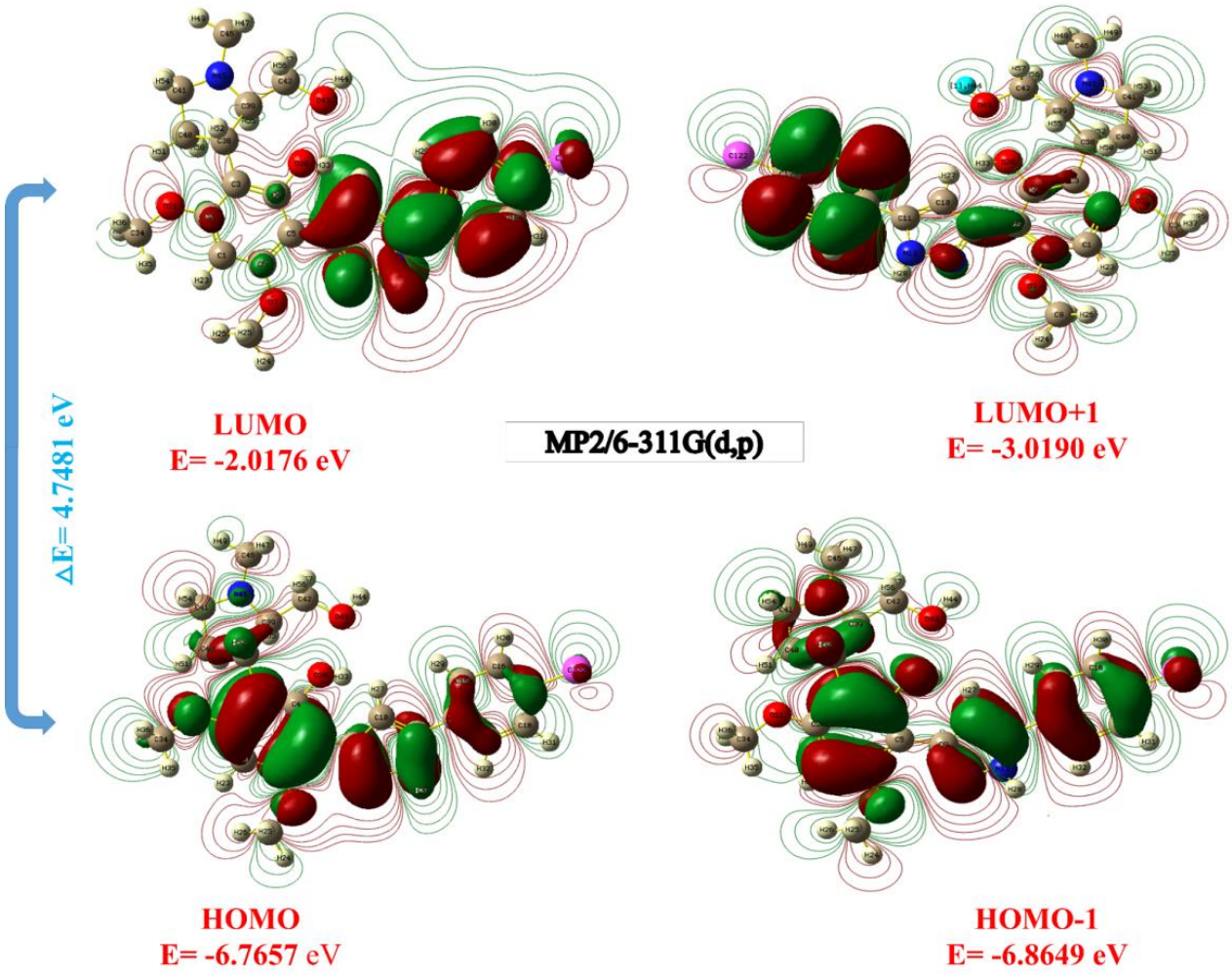

Figure 2. Boundary molecular orbitals of the HMP2 molecule using the 6-311G(d,p) basis set

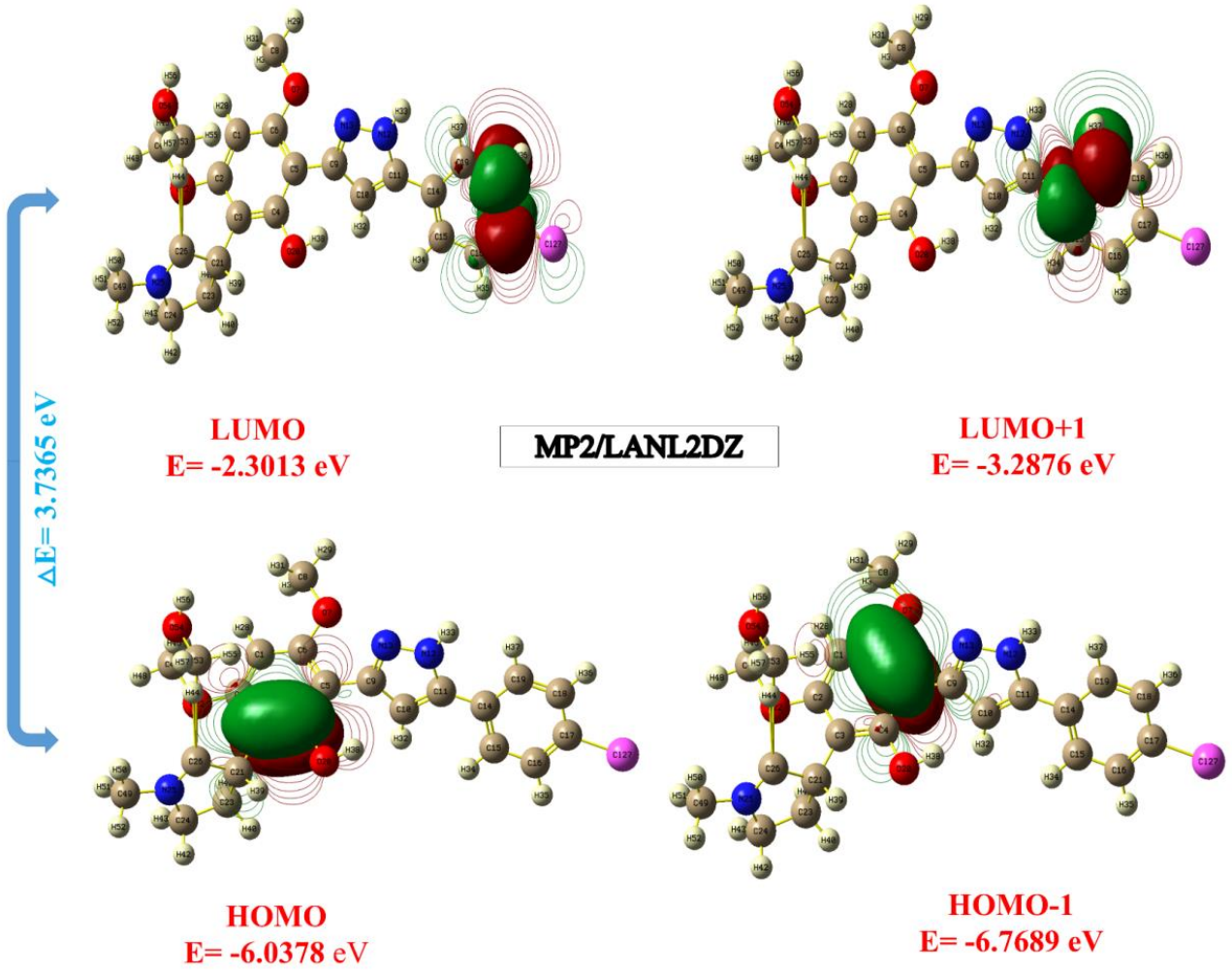

Figure 3. Boundary molecular orbitals of the HMP2 molecule using the LANL2DZ basis set

3.3. Molecular electrostatic potential (MEP)

Molecular electrostatic potential (MEP) mapping is an analytical method that allows the determination of chemically active regions of a molecule by projecting the electrostatic potential onto an isoelectron density surface (Gören et al., 2024b). This approach simultaneously visualizes the spatial dimensions and geometry of the molecule as well as its electrostatic potential distribution. In the color scale used in MEP maps, red tones represent electron-rich and partially negative regions, blue tones represent electron-poor and partially positive regions; light blue indicates slight electron deficiency, yellow indicates slight electron density, and green indicates electrically neutral regions (Marinho & Marinho, 2016). Figure 4 shows the molecular electrostatic potential (MEP) maps of the HMP2 molecule calculated using the 6-311G(d,p) and LANL2DZ basis sets. The results obtained with two different basis sets reveal the changes in the electrostatic potential distribution on the molecular surface. In both calculations, red and orange colors represent electron-rich regions, i.e., regions with negative potential, while blue and light blue colors indicate positive potential, i.e., electron-poor regions. The red regions, concentrated especially around electronegative atoms such as oxygen and nitrogen, indicate that these regions are nucleophilic, while the blue regions around hydrogen atoms show electrophilic regions. Calculations using the 6-311G(d,p) basis set reveal a broader and more detailed distribution of the electrostatic potential. In contrast, maps obtained with the LANL2DZ basis set show smoother transitions and more limited potential differences. These differences provide information about the computational accuracy and level of detail of the basis sets used. Both maps show that the molecule contains regions with both positive and negative potentials in chemical interactions, providing important clues about the reactive behavior of HMP2.

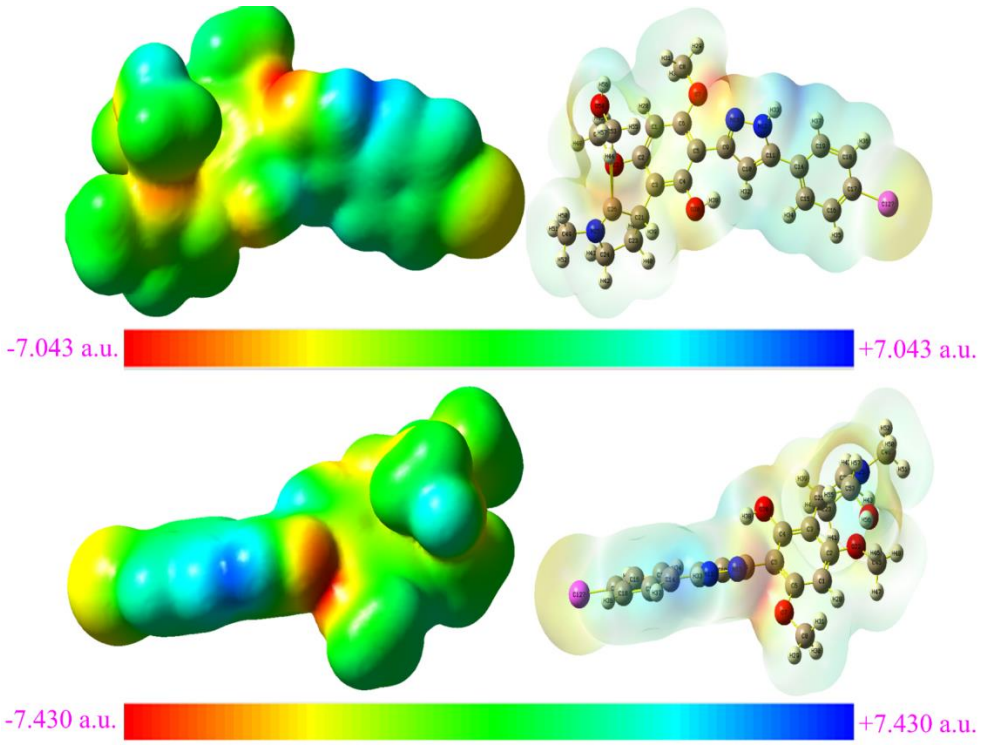

Figure 4. MEP map of HMP2 molecule calculated with basis sets 6-311G(d,p) and LANL2DZ.

3.4. Non-Linear optical properties (NLO)

Nonlinear optical (NLO) properties play a critical role in the development of electronic devices and optoelectronic applications. NLO properties are observed as changes in the optical behavior of molecules in the presence of an electromagnetic field, particularly in phase, amplitude, and frequency. To quantitatively study these molecular responses, several fundamental optical parameters are used. The mean polarizability ⟨α⟩ indicates how easily a molecule can be polarized by an applied electric field, while the polarizability anisotropy Δα describes the polarizability difference of the molecule in different spatial directions and is directly related to the molecular geometry (Asif et al., 2022). The total first-order hyperpolarizability βtotal measures first-order NLO responses of the molecule, such as second harmonic generation or electro-optical modulation, while the second-order hyperpolarizability γ reflects higher-order NLO responses, such as third harmonic generation. Furthermore, the dipole moment μ indicates the electrical asymmetry and polar nature of the molecule (Rasool et al., 2022). These parameters can be calculated using the relevant mathematical expressions. The mean polarizability ⟨α⟩ and anisotropy Δα are obtained from the polarizability tensor components of the molecule in the xyz coordinates, while βtotal is found by summing the squares of the components. These obtained values provide fundamental information for understanding the linear and nonlinear responses of the molecule to optical fields and for use in electronic applications (Waheed et al., 2021). NLO parameters were calculated using equations 1-4.

$$\mu = \left(\mu_x^2 + \mu_y^2 + \mu_z^2\right)^{1/2} \quad (1)$$

$$\alpha_{\text{Total}} = \frac{1}{3}(\alpha_{xx} + \alpha_{YY} + \alpha_{zz}) \quad (2)$$

$$\beta_{Total} = (\beta^2 x + \beta^2 y + \beta^2 z)^{1/2} \quad (3)$$

$$(\beta xxx + \beta xyy + \beta xzz)^2 + (\beta yyy + \beta yxx + yzz)^2 + (\beta zzz + \beta zxx + \beta zyy)^2]^{\frac{1}{2}} \quad (4)$$

The electrical properties and nonlinear optical (NLO) parameters of the HMP2 molecule, calculated using the 6-311+G(d,p) and LANL2DZ basis sets, have been summarized in Table 4. Calculations were performed to determine the polar nature, polarizability, and hyperpolarizability of the molecule. The calculated dipole moments show that the molecule has a strong polar character. $\mu_{(D)}$ was found to be 4.223 D in the 6-311+G(d,p) basis set and 4.933 D in the LANL2DZ basis set. These values indicate that the molecule exhibits a distinct directional electrical moment with both basis sets and has a high sensitivity to electric

fields. Specifically, the μx component is dominant, and the molecule is observed to exhibit a tendency towards directional polarization along the x-axis. The polarizability of the molecule is an indicator of its linear response to external electric fields. The calculated components show that the α_{zz} value is higher than the other components, indicating that the molecule is more flexible and more sensitive to polarization along the z-axis. Both basis sets yielded similar α values (α(au) -144, -147), revealing that the sensitivity of the calculations to the basis set is limited. Hyperpolarizability determines the second-order nonlinear optical response of the molecule and is particularly important in optoelectronic applications. Examining the table, it is seen that the β_{XXX} component is dominant and has a negative sign. This indicates that the molecule has a strong second-order NLO response along the x-axis. The other components are small with $\beta_{(esu)}$ values of $2.43–2.46\times10^{-30}$ esu, revealing that the NLO efficiency of the molecule is anisotropic. The calculations show that the results of the 6-311+G(d,p) and LANL2DZ basis sets are quite close to each other. This indicates that the NLO properties of the HMP2 molecule are not significantly affected by the basis set change, and both methods provide reliable predictions. The obtained NLO parameters reveal that the HMP2 molecule exhibits a moderately strong nonlinear optical response. In particular, the high dipole moment and the dominant β_{XXX} component suggest that the molecule could be a potential candidate for optical modulation, frequency conversion, and electro-optical applications. The fact that the polarizability and hyperpolarizability values are independent of the basis set supports the idea that these properties of the molecule are also experimentally predictable.

Table 4. NLO parameters of HMP2 molecule calculated using 6-311+G(d,p) and LANL2DZ basis sets

Parameters	6-311+G(d,p)	LANL2DZ	Parameters	6-311+G(d,p)	LANL2DZ
μ_x	-3.8395	3.8754	β_{XXX}	-281.0580	-279.2704
μ_y	-1.7495	1.8044	β_{YYY}	-19.8891	-21.3294
μ_z	0.1760	0.2090	β_{ZZZ}	4.1114	3.9632
$\mu_{(D)}$	4.2229	4.9331	β_{XYY}	-44.7023	-43.1716
α_{xx}	-177.8939	-178.7535	β_{XXY}	-123.6483	122.8834
α_{YY}	-170.5959	-171.7255	β_{XXZ}	-30.4501	-31.9146
α_{zz}	-196.4998	-197.9006	β_{XZZ}	-36.5791	-35.8134
α_{XY}	10.3072	12.5036	β_{YZZ}	13.1892	-14.1224
α_{XZ}	8.3093	8.4450	β_{YYZ}	15.6921	16.8025
α_{YZ}	-8.8943	-7.7221	β_{XYZ}	-2.7594	-3.0630
α(au)	-144.1229	-147.4356	β(esu)	$2.43x10^{-30}$	$2.46x10^{-30}$

3.5. Mulliken atomic charges

Mulliken charge analysis is a traditional method aimed at quantitatively determining the electron distribution between atoms in molecules. This method calculates the electron density in each atomic orbital using the molecule's wave function or electron density, and distributes the shared electrons equally among the respective atoms (Parandekar et al., 2008). Thus, the total charge of each atom is determined, providing information about the charge distribution in the molecule. Mulliken charges can be used to study the character of bonds between atoms and the reactive regions of the molecule; for example, atoms with high electron density may be more nucleophilic, while those with low density may be more electrophilic. Although this method is quick and easy to calculate, it is sensitive to the base set and method used, so charge values may vary in different calculations. Mulliken charge analysis is an important tool in understanding the electrical properties, dipole moments, and chemical bonding characteristics of molecules (Satheeshkumar et al., 2022). When the Mulliken atomic charges of the HMP2 molecule are examined (Table 5), it is observed that the electron distribution generally differs depending on the type of atom. While carbon atoms take on both small positive and negative charges, it is understood that the electron density is irregular according to the bonds of the molecule. Oxygen atoms generally carry negative charges, reflecting their high electronegativity and electron-attracting capacity; however, the observation of a positive charge in the O43 atom with the LANL2DZ basis set indicates that different basis sets predict electron distribution differently. The halogen Cl22 carries a slightly negative charge, revealing that the electron density is balanced depending on the chlorine atom's bonds. Hydrogen atoms mostly carry positive charges, showing that they lose electron density to the electronegative atoms they bond to. When comparing two different basis sets, it is understood that the 6-311+G(d,p) basis set gives more precise and balanced charges, while with LANL2DZ, some atoms show sign changes and magnitude differences. A sign change was observed in the C38 atom and a large charge difference in the O43 atom. This shows that different basis sets can interpret electron density

differently, especially in complex molecules containing heteroatoms. In conclusion, the HMP2 molecule has a polar structure, with negative charges generally concentrated on oxygen and nitrogen atoms, while positive charges are found on hydrogen and some carbon atoms, which plays a significant role in determining the molecule's chemical reactivity and polarity.

Table 5. Mulliken atomic charges of HMP2 molecule

ATOM	6-311+G(d,p)	LANL2DZ	ATOM	6-311+G(d,p)	LANL2DZ
C1	-0.174	-0.197	O20	-0.466	-0.408
C2	0.281	0.301	O21	-0.435	-0.403
C3	-0.013	-0.055	Cl22	-0.088	-0.136
C4	0.274	0.255	C34	-0.009	-0.087
C5	-0.117	-0.154	C38	0.096	-0.120
C6	0.302	0.220	C42	0.092	-0.069
O7	-0.464	-0.468	O43	-0.559	0.427
C8	-0.020	-0.090	H23	0.180	0.220
O9	0.270	0.330	H26	0.096	0.172
C10	-0.232	-0.240	H27	0.118	0.140
C11	0.254	-0.280	H28	0.238	0.210
N12	-0.408	-0.370	H29	0.121	0.151
N13	-0.268	-0.328	H30	0.135	0.156
C14	-0.089	-0.033	H31	0.132	0.146
C15	-0.079	-0.071	H32	0.133	0.182
C16	0.008	-0.036	H24	0.165	0.211
C18	-0.003	0.013	H25	0.096	0.100

3.6. NBO analysis

Natural Bonding Orbital (NBO) analysis is a powerful tool for identifying individual bonds and borrowed electron pairs that play a critical role in chemical reactions. This method describes the phenomenon known as "delocalization correction to the zero-order Lewis structure", starting from localized NBOs of the ideal Lewis structure; this process is analyzed through the interactions of filled donor and empty acceptor orbitals that lead to the loss of occupancy of non-Lewis empty orbitals (Sakthivel et al., 2018). Using second-order perturbation theory, the stabilization energy E(2) due to electron delocalization is calculated for each donor (i) and acceptor (j) NBO pair (Singh et al., 2018). This analysis provides a quantitative assessment of bond-counterbond interactions in the molecule, and the results based on the Fock matrix on the NBO basis have been summarized in Table 6.

$$E^{(2)} = -n_i \cdot \frac{(Fij)^2}{\mathcal{E}_j - \mathcal{E}i} \tag{5}$$

When we look at the table, it is the NBO (Natural Bond Orbital) analysis of the HMP2 molecule with the 6-311+G(d,p) basis set and shows the interactions of electron pairs in the molecule, i.e. electron density transfer and bond stability. The occupancy values of π and σ bonds are generally in the range of 1.8–1.99 and the second-order energy (E(2)) has been calculated through electron density transfer to antibonding (σ* or π*) orbitals. E(2) values represent the contribution of electron transfer from one orbital to another to molecular stability; the higher the value, the stronger the interaction and the more stable the molecule. The C1–C2 π→C5–C6 π* interaction shows a very high value of 23.98 kcal/mol, which indicates that there is a strong delocalization between π systems in the molecule and that aromatic or conjugated structures contribute to electron stabilization. Similarly, the C3–C4 π→C1–C2 π* and C5–C6 π→C3–C4 π* interactions are around 24 kcal/mol, indicating that the π electrons are well delocalized throughout the molecule. Significant interactions also exist between σ bonds. The C1–C6 σ→C2–O21 σ* interaction has an energy of 5.78 kcal/mol, suggesting that σ bonds contribute moderately to molecular stability by providing antibonding orbitals. Similarly, the C1–H23 σ→C34–H35 σ* interaction offers a slightly higher energy contribution of 8.53 kcal/mol. Bonds involving nitrogen and oxygen also exhibit significant interactions. The C39–N45 π→C42–O43 π* interaction shows strong π delocalization at 18.98 kcal/mol. This indicates that there is also electron density transfer between the heteroatoms of the molecule, increasing molecular stability. Furthermore, some σ–σ* interactions are noteworthy; the N12–N13 σ→C5–C9 σ* interaction has

an energy of 6.98 kcal/mol. This shows that partial electron transfer to the antibonding orbitals of σ bonds supports the flexibility and stability of the molecule. It reveals that the HMP2 molecule has dense electron delocalization between both π and σ systems, with strong resonance and bond stability effects, especially in π systems. The molecule has an energy-optimized electron distribution through both carbon-carbon and heteroatom bonds.

Table 6. NBO values calculated for HMP2 molecule using the LANL2DZ basis set

NBO(i)	Type	Occupancies	NBO(j)	Type	Occupancies	E(2)a (Kcal/mol)	E (j)-E(i)b (a.u.)	F (i, j)c (a.u)
C1-C2	π	1.85882	C5-C6	π*	1.98684	23.98	0.58	0.108
C1- C6	σ	1.97330	C2-O21	σ*	1.98684	5.78	1.37	0.079
C1-H23	σ	1.96746	C34-H35	σ*	1.98770	8.53	1.42	0.099
C2-C3	σ	1.96900	C1-C2	σ*	1.97990	4.14	1.73	0.076
C3-C4	π	1.81910	C1-C2	π*	1.85882	24.79	0.55	0.105
C3-C38	σ	1.97725	C3-C4	σ*	1.97308	5.57	1.74	0.088
C4-C5	σ	1.97225	C3-C38	σ*	1.97725	5.21	1.46	0.078
C4-O20	σ	1.99200	C2-C3	σ*	1.96900	3.44	1.72	0.069
C5-C6	π	1.97477	C3-C4	π*	1.81910	24.27	0.57	0.106
C5-C9	σ	1.97320	C5-C6	σ*	1.97477	4.86	1.74	0.053
C8-H24	σ	1.99208	C6-O7	σ*	1.98806	4.34	0.31	0.066
C9-C10	σ	1.97511	C10-C11	σ*	1.97753	4.06	1.75	0.075
C9-N13	π	1.93710	C10-C11	π*	1.88597	10.15	0.64	0.073
C10-C11	π	1.97753	C9-N13	π*	1.93710	27.15	0.58	0.114
C10-H27	σ	1.97636	O20-H23	σ*	1.98685	5.09	1.47	0.077
C11-N12	σ	1.98722	C10-H27	σ*	1.97636	4.90	1.64	0.080
N12-N13	σ	1.98170	C5-C9	σ*	1.97320	6.98	1.63	0.095
C14-C15	π	1.81924	C16-C17	π *	1.85267	19.75	0.54	0.093
C15-C16	σ	1.97075	C17-Cl22	σ*	1.98821	7.82	1.18	0.086
C16-C17	π	1.85267	C14-C15	π *	1.81924	17.67	0.59	0.092
C16-H30	σ	1.98247	C17-C18	σ*	1.98102	6.71	1.35	0.085
C18-C19	π	1.97931	C14-C15	π*	1.81924	19.29	0.57	0.094
C39-N45	π	1.93466	C42-O43	π*	1.99427	18.98	1.12	0.131
C41-N45	σ	1.95652	C39-N45	σ*	1.93466	7.52	0.83	0.071

3.7. Molecular docking analysis

Molecular docking is an effective method widely used in computer-aided drug design that allows the prediction of interactions between biologically active small molecules and target proteins. This approach enables the evaluation of ligand-protein binding modes and binding affinities, allowing for an understanding of the therapeutic potential of compounds at the molecular level (Rahuman et al., 2020). Therefore, molecular docking studies play a critical role in identifying potential candidate molecules in drug discovery and development processes. Inflammatory pain plays a significant role in the pathogenesis of many chronic diseases, and inhibition of target proteins involved in this process is considered an effective treatment strategy (Ugwu et al., 2018). In this study, the binding modes and affinities of the HMP2 compound against the inflammatory pain-related target proteins PDB ID: 3LN1 and PDB ID: 6COX were investigated using molecular docking analyses. Three-dimensional crystal structures of the target proteins were obtained from the Protein Data Bank (3LN1 (Bank, 2013); 6COX (Bank, 2017)), and docking studies were performed using AutoDock Vina software (Eberhardt et al., 2021). According to the obtained docking results, it was determined that the HMP2 compound exhibited negative binding energies with both target proteins and could form stable complexes. In particular, the lower docking score obtained for PDB ID: 6COX indicates that HMP2 has a higher binding affinity towards this target. Molecule-protein interactions were analyzed using the Discovery Studio Visualizer program (BIOVIA, 2016), and it was observed that hydrogen bonds, van der Waals interactions, and π-alkyl, π-sigma, and π-sulfur interactions contributed to complex stability.

Comparison of interaction types and bond lengths for both complexes revealed that van der Waals and alkyl/π-alkyl interactions predominated, with HMP2 appropriately positioned in hydrophobic binding sites. Longer-range and relatively weaker interactions were observed in the complex formed with PDB ID: 3LN1, while conventional hydrogen bonds formed with PRO-154 and GLU-465 in the PDB ID: 6COX complex

presented stronger and shorter-range interactions. These findings support the idea that HMP2 has a stronger and more stable binding profile, particularly with the 6COX enzyme.

The anti-inflammatory potential of the HMP2 compound can be attributed to the different pharmacophore groups present in its structure. The 1H-pyrazole ring within the molecule is one of the important heterocyclic skeletons strongly associated with cyclooxygenase-2 (COX-2) enzyme inhibition in the literature. Several studies have reported that pyrazole derivatives inhibit prostaglandin synthesis by binding to the COX-2 active site and thus exert an anti-inflammatory effect (Penning et al., 1997; Ju et al., 2022). Therefore, the pyrazole ring of HMP2 is considered a key pharmacophore in terms of interaction with the COX-2 target. The 4-chlorophenyl group in the structure enhances its lipophilic character, facilitating binding to the hydrophobic regions of target proteins and supporting ligand-protein binding affinity. It has been reported in the literature that halogen substituents enhance hydrophobic pocket interactions and increase biological activity in COX enzyme inhibitors (Meanwell, 2011; Lu et al., 2012). The 2-hydroxymethyl-1-methylpyrrolidine group in the molecule can act as a hydrogen bond donor and acceptor and can form stable interactions with polar amino acid residues (e.g., GLU and PRO) in the protein active site. This is consistent with hydrogen bond interactions observed in docking analyses (Ghoneim et al., 2025). In addition, the 3,5-dimethoxyphenol group strengthens π–π and π-alkyl interactions by increasing the electron density of the aromatic system thanks to its electron-donating effect and contributes to complex stability. It is known that phenolic structures exhibit antioxidant and free radical scavenging properties in inflammatory processes (Ewieda et al., 2023; Hawash et al., 2025).

In general, literature data indicate that heterocyclic structures containing pyrazole, phenolic, and halogen-containing aromatic systems can exhibit anti-inflammatory activity through COX-2 inhibition and suppression of inflammatory pathways. In this context, when the structural properties and molecular docking results of the HMP2 compound are evaluated together, it is predicted that it may exhibit anti-inflammatory potential, especially by establishing strong and stable interactions with the COX-2 enzyme (Ju et al., 2022).

Table 7. Docking scores against PDB:3LN1 and PDB: 6COX enzymes of HMP2 compound

Compound	Docking Score (kcal/mol)	
	PDB:3LN1	PDB: 6COX
HMP2	-8.60	-8.80

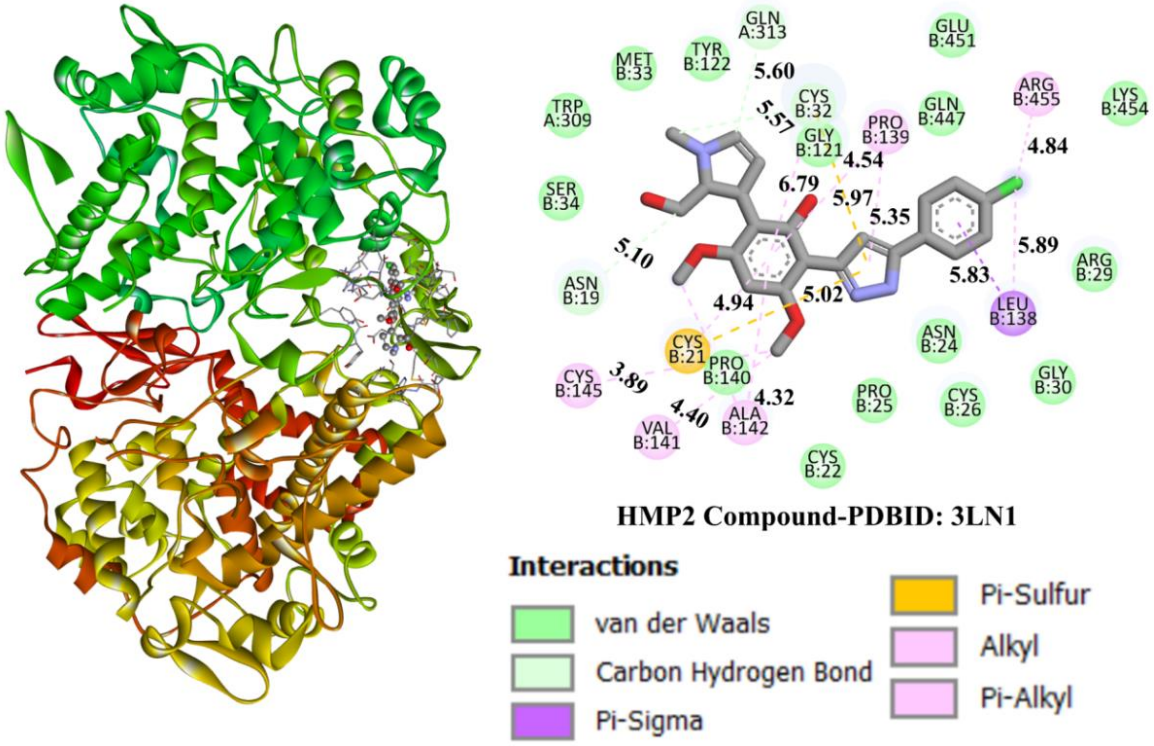

Figure 5. 2D and 3D images of the HMP2 compound and PDB: 3LN1 protein

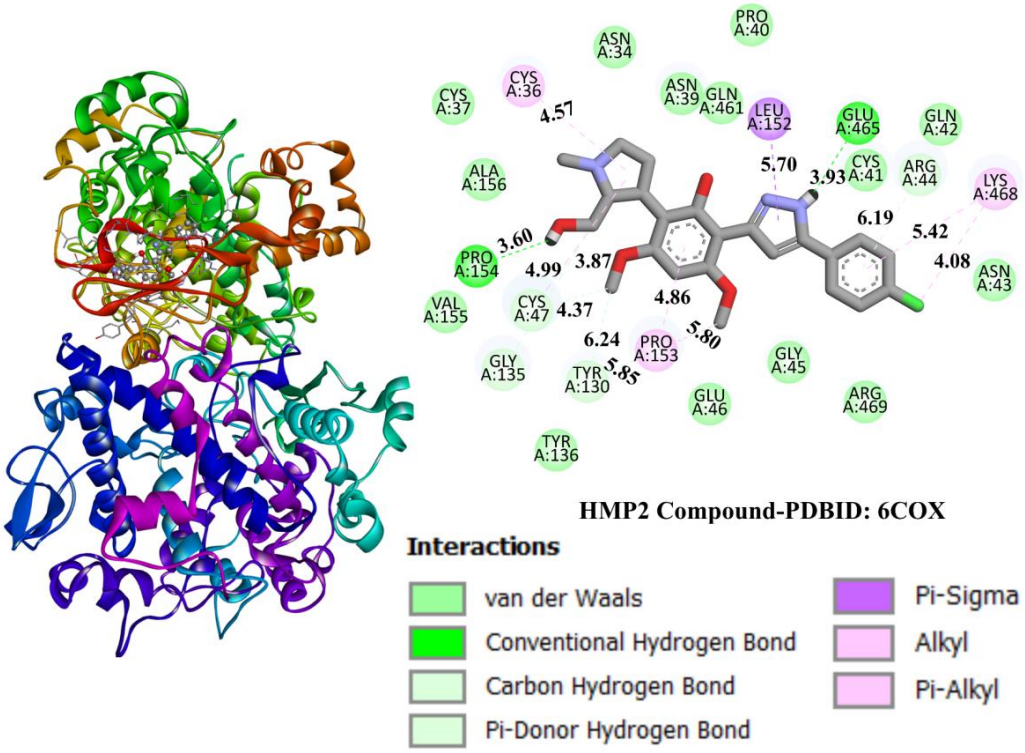

Figure 6. 2D and 3D images of the HMP2 compound and PDB: 6COX protein

Table 8. The interaction parameters between HMP2 compound and PDB: 3LN1 and PDB: 6COX enzymes

Type of Bond	HMP2 compound PDB: 3LN1	Bond Length (Å)	HMP2 compound PDB: 6COX	Bond Length (Å)
Van der Waals Interactions	MET-33	-	CYS-37	-
	TYR-122	-	ALA-156	-
	SER-34	-	GLY-135	-
	GLN-313	-	LYS-403	-
	LYS-454	-	TYR-449	-
Carbon Hydrogen Bond	GLN-313	5.60	CYS-47	4.37
	CYS-32	5.57	TYR-130	6.24
	ASN-19	5.10		
Pi-Sigma	Leu-138	5.83	LEU-152	5.70
Alkyl	PRO-139	4.54, 5.35	LYS-468	4.08, 5.42
	ARG-455	4.84	CYS-36	4.57
	LEU-138	5.89		
Pi–Alkyl	CYS-145	3.89	PRO-153	4.86
	VAL-141	4.40		
	ALA-142	4.32		
Conventional Hydrogen Bonds	-	-	PRO-154	3.60
	-	-	GLU-465	3.93
Pi-Donor Hydrogen Bond	-	-	GLN-42	6.19

3.8. ADMET analysis

In the drug development process, it is not sufficient for candidate compounds to merely demonstrate target-specific biological activity; they must also possess appropriate pharmacokinetic and toxicological properties (Ojuka et al., 2023). ADMET (Absorption, Distribution, Metabolism, Elimination, Toxicity) parameters play a decisive role in this regard (Abchir et al., 2023). When the physicochemical and ADMET profile of the HMP2 compound (Table 9) is examined, some positive characteristics are observed, along with significant limitations. The molecular weight (443.16 g/mol) conforms to the Lipinski criteria, but high molecular weight can negatively affect absorption and distribution. Values of nHA=7, nHD=3, and TPSA=90.84 Å² indicate generally good bioavailability potential due to sufficient hydrogen bonding capacity and the absence

of excessive polarity. The LogP value (3.863) indicates moderate lipophilicity, which provides an advantage in terms of membrane permeability, but high PPB (96.38%) may lead to a decrease in the free fraction. HIA (0.011) and Caco-2 (-5.026) values indicate poor oral absorption; therefore, formulation or structural optimization is necessary. The BBB value (0.623) suggests moderate brain penetration, while VD (1.599 L/kg) and high PPB may be limiting factors in distribution. In terms of metabolism, inhibition of CYP2D6 (0.900) and CYP3A4 (0.815) increases the risk of possible interactions. The T½ value (0.14) indicates a short half-life, which may require more frequent dosing. In terms of toxicity, hERG blockade (0.78) carries a risk of serious cardiotoxicity; H-HT (0.219), AMES (0.259), and rat acute toxicity (0.267) are moderate. Therefore, structural optimization and appropriate formulation strategies are recommended in the development of HMP2 to increase bioavailability, reduce metabolic interactions, and minimize cardiotoxicity.

Table 9. The HMP2 compounds's physicochemical, lipophilicity and ADMET parameters

Property	HMP2
Molecular Weight	443.16
nHA	7
nHD	3
logP	3.863
TPSA	90.84
HIA	0.011
Caco-2 Permeability	-5.026
BBB	0.623
PPB	96.38%
VD	1.599
CYP2D6	0.9
CYP3A4	0.815
$T_{1/2}$	0.14
hERG Blockers	0.78
H-HT	0.219
AMES Toxicity	0.259
Rat Oral Acute Toxicity	0.267

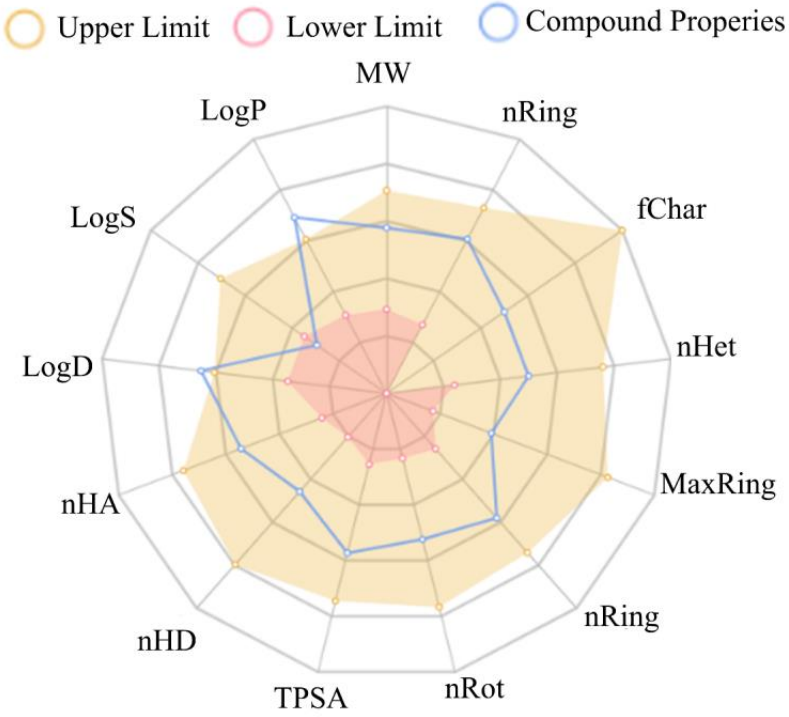

Figure 7. Color regions and physicochemical parameters of HMP2 compound

4. Conclusion

This allows for the classification of the structural, electronic, and biological properties of HMP2 protection in silico. Symmetric replicates at the MP2 level reveal that HMP2 possesses a stable and largely plane-like geometry. The results obtained with both the 6-311G(d,p) and LANL2DZ basis sources are generally consistent, with the longer bond lengths calculated with LANL2DZ suggesting systematic aspects that may arise from the limited and effective nuclear potential of the basis set. This finding highlights that basis set choices can have significant effects on results, especially in the characterization of heteroatom-containing systems. HOMO–LUMO analyses indicate a wider range of energy members and thus higher stability in the 6-311G(d,p) basis set, while the LANL2DZ basis set shows narrower energy particles and higher electron affinity values, resulting in a more reactive character of HMP2. MEP and Mulliken charge analyses revealed the presence of nucleophilic regions concentrated around oxygen and nitrogen atoms, and electrophilic regions along hydrogen atoms; furthermore, significant effects of ground set selections on charge states and electrostatic potential were demonstrated. NBO analyses confirmed that HMP2 possesses a wide resonance network with strong π–π* and σ–σ* delocalizations, thus providing good stabilization in terms of flexibility. Optoelectronic NLO programming revealed that HMP2 exhibits a strong polar character with a high dipole moment and pronounced polarization values. The dominance of βxxx in hyperpolarizability formation indicates that the molecule exhibits a second-order optical reaction, particularly along the x distribution. These results suggest that HMP2 can be evaluated not only for pharmaceutical potential monitoring but also for optoelectronic applications. Molecular docking studies reveal that HMP2 exhibits significant affinity for the proteins PDB:3LN1 and PDB:6COX, which target the development of inflammatory pain. In particular, the docking score of –8.80 kcal/mol and short-range hydrogen bonds obtained with the 6COX protein support HMP2 as a potential inhibitor candidate against this target. However, ADMET analyses have shown that its pharmacokinetic profile can be determined within certain limits. Low HIA and CaCO-2 permeability, high plasma protein binding, CYP2D6 and CYP3A4 inhibitory activity, and possible hERG blockade are points that require careful evaluation, especially in terms of oral bioavailability and protective safety. In conclusion, the findings indicate that HMP2 is a molecule with potential anti-inflammatory activity. However, further improvement efforts require structural modification and strengthening of the appropriate formulation to support oral absorption, minimize metabolic linkages, and reduce hERG intensity. Accordingly, in vitro and in vivo biological evaluations of HMP2 are essential as a crucial next step to more clearly define the molecule's drug candidacy.

Acknowledgement

The authors sincerely thank the Editor and Reviewers for their valuable comments and contributions during the evaluation process of the manuscript.

Author contribution

Ercan Avınç contributed to data collection, quantum chemical calculations, molecular docking studies, formal analysis, visualization, and preparation of the original draft of the manuscript. Kenan Gören contributed substantially to the conceptualization and design of the study, methodology, supervision, validation, interpretation of the results, and critical revision of the manuscript. Ümit Yıldıko contributed to data analysis, validation, literature review, and manuscript revision.

Declaration of ethical code

The authors of this article declares that this study does not require ethical committee approval or legal permission.

Conflict of Interest

The authors declare that there is no competing interest

References

Abchir, O., Yamari, I., Nour, H., Daoui, O., Elkhattabi, S., Errougui, A., & Chtita, S. (2023). Structure-based Virtual Screening, ADMET analysis, and molecular dynamics simulation of Moroccan natural compounds as candidates α-amylase inhibitors. *ChemistrySelect*, 8(26), e202301092.

ADMETlab2.0. A platform for systematic ADMET evaluation. Retrieved 31.01.2026 from https://admetmesh.scbdd.com/

Agbektas, T., Coskun, H., Genc, H. C., Cinar Kaya, G., Tas, A., Goren, K., Huseynzada, A., Guliyev, R., Hasanova, U., Kaya, S., Morales-Bayuelo, A., & Silig, Y. (2026). Evaluation of the Anticancer Effects of DODP on Gene Expression and Oxidative Stress in Gastric Cancer: An Integrated Docking, Bioinformatics, and Experimental Approach. *Life*, 16(4), 534.

Anwer, K. E., Abdelgawad, M. A., Abd El-Sattar, N. E., El-Morsy, A., Nasr, T., Elmowafy, M., El-Adl, K., & Ahmed, N. M. (2026). Pyrazole/pyrimidine derivatives endowed with azobenzenes as dual EGFR T790M and VEGFR-2 inhibitors: anticancer, docking, synthesis, design and ADMET assessments. *RSC advances*, 16(13), 11458–11477.

Asif, A., Maqsood, N., Tamam, N., Ayub, K., Ans, M., Iqbal, J., Al-Buriahi, M., Alomairy, S., & Alrowaili, Z. (2022). DFT study of transition metals doped calix-4-pyrrole with excellent electronic and non-linear optical properties. *Computational and Theoretical Chemistry*, 1214, 113767.

Aysha, M., Selvam, K., Adhavan, R., Prakash, P., & Shivakumar, M. S. (2026). Investigating the therapeutic properties of Dolichandrone falcata leaves: Anti-inflammatory effects, acetylcholinesterase inhibition and in silico docking against snake venom proteins. *Journal of Molecular Structure*, 1359, 145449. https://doi.org/https://doi.org/10.1016/j.molstruc.2026.145449

Bağlan, M., Gören, K., & Çakmak, İ. (2022). Theoretical Investigation of ^{1}H and ^{13}C NMR Spectra of Diethanol Amine Dithiocarbamate RAFT Agent. *Journal of the Institute of Science and Technology*, 12(3), 1677–1689. https://doi.org/10.21597/jist.1103750

Bağlan, M., Gören, K., Tahiroğlu, V., Kotan, G., Manap, S., & Yüksek, H. (2026). Design, Synthesis, DFT-Based Characterization, Molecular Docking, and ADMET Evaluation of a Novel Mannich Base Derivative. *ChemistrySelect*, 11(9), e06617.

Bağlan, M., Gören, K., & Yıldıko, Ü. (2023a). DFT Computations and Molecular Docking Studies of 3-(6-(3-aminophenyl) thiazolo [1, 2, 4] triazol-2-yl)-2H-chromen-2-one (ATTC) Molecule. *Hittite Journal of Science and Engineering*, 10(1), 11–19.

Bağlan, M., Gören, K., & Yıldıko, Ü. (2023b). HOMO–LUMO, NBO, NLO, MEP analysis and molecular docking using DFT calculations in DFPA molecule. *International Journal of Chemistry and Technology*, 7(1), 38–47. https://doi.org/10.32571/ijct.1135173

Bağlan, M., Yıldıko, Ü., & Gören, K. (2023). DFT Calculations and Molecular Docking Study ın 6-(2”-Pyrrolidinone-5”-Yl)-(-) Epicatechin Molecule From Flavonoids. *Eskişehir Teknik Üniversitesi Bilim ve Teknoloji Dergisi B - Teorik Bilimler*, 11(1), 43–55. https://doi.org/10.20290/estubtdb.1126604.

Bank, P. D. (2013). Structure of celecoxib bound at the COX-2 active site. *Protein Data Bank*. Retrieved 31.01.2026 from https://www.rcsb.org/structure/3LN1.

Bank, P. D. (2017). Cyclooxygenase-2 (Prostaglandin Synthase-2) Complexed with a Selective Inhibitor, SC-558 IN I222 SPACE GROUP. *Protein Data Bank*. Retrieved 31.01.2026 from https://www.rcsb.org/structure/6COX.

BIOVIA, D. S. (2016). Discovery Studio Visualizer. *In Dassault Systèmes*.

Cherian, R. M., & Ravikumar, C. (2026). Spectroscopic analysis, DFT and molecular docking study of potent antibacterial agent 4- hydroxy-8-methoxy quinoline-3-carboxylic acid ethyl ester. *Chemical Physics Impact*, 101064. https://doi.org/https://doi.org/10.1016/j.chphi.2026.101064.

Cremer, D. (2011). Møller–Plesset perturbation theory: from small molecule methods to methods for thousands of atoms. *Wiley Interdisciplinary Reviews: Computational Molecular Science*, 1(4), 509–530.

Çimen, E., Gören, K., Tahiroğlu, V., & Bağlan, M. (2026). Chemical reactivity, molecular docking and ADMET profile of (E)-4-((2-butyl-5-(2-carboxy-3-(thiophen-2-yl)prop-1-en-1-yl)-1H-imidazol-1-yl)methyl)benzoic acid molecule: evaluation as a diabetes drug candidate. *Journal of the Iranian Chemical Society*, 23(2), 46. https://doi.org/10.1007/s13738-026-03347-8.

Deshmukh, H. S., Adole, V. A., Frit, A. A. P., Mali, S. N., Yasin, H. K. A., Patil, B. N., Janani, S., & Jagdale, B. S. (2025). Synthesis, characterization, computational and biological evaluation of pyrazole hydrazones as promising anti-inflammatory agents. *Scientific Reports*, 15(1), 42206. https://doi.org/10.1038/s41598-025-26088-9.

Eberhardt, J., Santos-Martins, D., Tillack, A. F., & Forli, S. (2021). AutoDock Vina 1.2. 0: new docking methods, expanded force field, and python bindings. *Journal of chemical information and modeling*, 61(8), 3891–3898.

Ewieda, S. Y., Ahmed, E. M., Hassan, R. A., & Hassan, M. S. A. (2023). Pyridazine derivatives as selective COX-2 inhibitors: A review on recent updates. Drug Dev Res, 84(8), 1595–1623. https://doi.org/10.1002/ddr.22118.

G.W.T. M.J. Frisch, H. B. S., G.E. Scuseria, M.A. Robb, J.R. Cheeseman, G. Scalmani, V. Barone, B. Mennucci, G.A. Petersson, H. Nakatsuji, M. Caricato, X. Li, H.P. Hratchian, A.F. Izmaylov, J. Bloino, G. Zheng, J.L. Sonnenberg, M. Hada, M. Ehara, K. Toyota, R. Fukuda, J. Hasegawa, M. Ishida, T. Nakajima, Y. Honda, O. Kitao, H. Nakai, T. Vreven, J.A. Montgomery Jr., J.E. Peralta, F. Ogliaro, M. Bearpark, J.J. Heyd, E. Brothers, K.N. Kudin, V.N. Staroverov, R. Kobayashi, J. Normand, K. Raghavachari, A. Rendell, J.C. Burant, S.S. Iyengar, J. Tomasi, M. Cossi, N. Rega, J.M. Millam, M. Klene, J.E. Knox, J.B. Cross, V. Bakken, C. Adamo, J. Jaramillo, R. Gomperts, R.E. Stratmann, O. Yazyev, A.J. Austin, R. Cammi, C. Pomelli, J.W. Ochterski, R.L. Martin, K. Morokuma, V.G. Zakrzewski, G.A. Voth, P. Salvador, J.J. Dannenberg, S. Dapprich, A.D. Daniels, Ö. Farkas, J.B. Foresman, J.V. Ortiz, J. Cioslowski, D.J. Fox. (2009). *Gaussian 09*. In (Version Revision A.02).

Ghoneim, M. M., Abdelgawad, M. A., Elkanzi, N. A. A., & Bakr, R. B. (2025). Review of the recent advances of pyrazole derivatives as selective COX-2 inhibitors for treating inflammation. *Mol Divers*, 29(2), 1789–1820. https://doi.org/10.1007/s11030-024-10906-9.

Gören, K., Bağlan, M., & Yıldıko, Ü. (2024a). Antimicrobial, and Antitubercular Evaluation with ADME and Molecular Docking Studies and DFT Calculatıons of (Z)-3-((1-(5-amino-1,3,4-thiadiazol-2-yl)-2-Phenylethyl)imino)-5-nitroindolin-2-one Schiff Base. *Karadeniz Fen Bilimleri Dergisi*, 14(4), 1694–1708. https://doi.org/10.31466/kfbd.1423367.

Gören, K., Bağlan, M., & Yıldıko, Ü. (2024b). Melanoma Cancer Evaluation with ADME and Molecular Docking Analysis, DFT Calculations of (E)-methyl 3-(1-(4-methoxybenzyl)-2,3-dioxoindolin-5-yl)-acrylate Molecule. *Journal of the Institute of Science and Technology*, 14(3), 1186–1199. https://doi.org/10.21597/jist.1467666.

Gören, K., & Yıldıko, Ü. (2024). Aldose reductase evaluation against diabetic complications using ADME and molecular docking studies and DFT calculations of spiroindoline derivative molecule. *Süleyman Demirel Üniversitesi Fen Bilimleri Enstitüsü Dergisi*, 28(2), 281–292.

Hawash, M., Shweiki, N., Qaoud, M. T., Çapan, I., Abualhasan, M., Kumar, A., Olech, B., & Dominiak, P. M. (2025). Trifluoromethyl–pyrazole–carboxamides as COX inhibitors: synthesis, microed structural analysis, computational profiling, and biological evaluation. *BMC Chemistry*, 19(1), 288. https://doi.org/10.1186/s13065-025-01659-z.

Ju, Z., Li, M., Xu, J., Howell, D. C., Li, Z., & Chen, F. E. (2022). Recent development on COX-2 inhibitors as promising anti-inflammatory agents: The past 10 years. *Acta Pharm Sin B*, 12(6), 2790–2807. https://doi.org/10.1016/j.apsb.2022.01.002.

Karrouchi, K., Yousfi, E. B., Sebbar, N. K., Ramli, Y., Taoufik, J., Ouzidan, Y., Ansar, M. h., Mabkhot, Y. N., Ghabbour, H. A., & Radi, S. (2017). New Pyrazole-Hydrazone Derivatives: X-ray Analysis, Molecular Structure Investigation via Density Functional Theory (DFT) and Their High In-Situ Catecholase Activity. *International Journal of Molecular Sciences*, 18(11), 2215.

Kotia, N., Verma, R., & Sinha, R. (2026). Vitex negundo L.: A comprehensive exploration of its phytochemistry, pharmacological attributes and molecular docking insights. *Pharmacological Research - Modern Chinese Medicine*, 18, 100762. https://doi.org/https://doi.org/10.1016/j.prmcm.2026.100762

Lu, Y., Liu, Y., Xu, Z., Li, H., Liu, H., & Zhu, W. (2012). Halogen bonding for rational drug design and new drug discovery. *Expert Opinion on Drug Discovery*, 7(5), 375–383. https://doi.org/10.1517/17460441.2012.678829

Marinho, E. S., & Marinho, M. M. (2016). A DFT study of synthetic drug topiroxostat: MEP, HOMO, LUMO. Int. J. Sci. Eng. Res, 7(8), 1264.

Meanwell, N. A. (2011). Improving drug candidates by design: a focus on physicochemical properties as a means of improving compound disposition and safety. *Chem Res Toxicol*, 24(9), 1420–1456. https://doi.org/10.1021/tx200211v.

Ojuka, P., Kimani, N. M., Apollo, S., Nyariki, J., Ramos, R. S., & Santos, C. B. (2023). Phytochemistry of plants in the genus Vepris: A review and in silico analysis of their ADMET properties. *South African Journal of Botany*, 157, 106–114.

Parandekar, P. V., Hratchian, H. P., & Raghavachari, K. (2008). Applications and assessment of QM: QM electronic embedding using generalized asymmetric Mulliken atomic charges. *The Journal of chemical physics*, 129(14).

Penning, T. D., Talley, J. J., Bertenshaw, S. R., Carter, J. S., Collins, P. W., Docter, S., Graneto, M. J., Lee, L. F., Malecha, J. W., Miyashiro, J. M., Rogers, R. S., Rogier, D. J., Yu, S. S., Anderson, G. D., Burton, E. G., Cogburn, J. N., Gregory, S. A., Koboldt, C. M., Perkins, W. E.,…Isakson, P. C. (1997). Synthesis and Biological Evaluation of the 1,5-Diarylpyrazole Class of Cyclooxygenase-2 Inhibitors: Identification of 4-[5-(4-Methylphenyl)-3- (trifluoromethyl)-1H-pyrazol-1-yl]benzenesulfonamide (SC-58635, Celecoxib). *Journal of Medicinal Chemistry*, 40(9), 1347–1365. https://doi.org/10.1021/jm960803q

Rahuman, M. H., Muthu, S., Raajaraman, B., Raja, M., & Umamahesvari, H. (2020). Investigations on 2-(4-Cyanophenylamino) acetic acid by FT-IR, FT-Raman, NMR and UV-Vis spectroscopy, DFT (NBO, HOMO-LUMO, MEP and Fukui function) and molecular docking studies. *Heliyon*, 6(9).

Ram, I. M., Maheta, J. B., Lakhnotra, D. K., Shaikh, N. H., Majethiya, V. U., & Bhola, Y. O. (2026). Design and synthesis of benzofuran–pyrazole–triazole hybrids via click chemistry: Antimicrobial, anticancer, ADMET, docking, and DFT studies. *Synthetic Communications*, 56(7), 537–564. https://doi.org/10.1080/00397911.2026.2642776

Rasool, A., Zahid, S., Alfryyan, N., Ayub, A. R., Ayub, K., Akhter, M. S., Iqbal, J., Al-Buriahi, M. S., & Yousef, E. S. (2022). Remarkable non-linear optical properties of gold cluster doped graphyne (GY): A DFT study. *Journal of Molecular Graphics and Modelling*, 114, 108204. https://doi.org/https://doi.org/10.1016/j.jmgm.2022.108204

Sakthivel, S., Alagesan, T., Muthu, S., Abraham, C. S., & Geetha, E. (2018). Quantum mechanical, spectroscopic study (FT-IR and FT-Raman), NBO analysis, HOMO-LUMO, first order hyperpolarizability and docking studies of a non-steroidal anti-inflammatory compound. *Journal of Molecular Structure*, 1156, 645–656.

Satheeshkumar, R., Prabha, K., Vennila, K. N., Sayin, K., Güney, E., Kaminsky, W., & Acevedo, R. (2022). Spectroscopic (FT-IR, NMR, single crystal XRD) and DFT studies including FMO, Mulliken charges, and Hirshfeld surface analysis, molecular docking and ADME analyses of 2-amino-4′-fluorobenzophenone (FAB). *Journal of Molecular Structure*, 1267, 133552. https://doi.org/https://doi.org/10.1016/j.molstruc.2022.133552

Sharma, N., Yadav, T., Kaur, N., Khandelwal, K., Pal, S. K., & Mathpati, R. S. (2026). Novel sulfonamide-linked pyrazoles: Synthesis, X-ray crystal structure, DFT, molecular docking, molecular dynamics simulations, ADMET analyses and antimicrobial activity. *Journal of Molecular Structure*, 1363, 145763. https://doi.org/https://doi.org/10.1016/j.molstruc.2026.145763

Singh, P., Islam, S., Ahmad, H., & Prabaharan, A. (2018). Spectroscopic investigation (FT-IR, FT-Raman), HOMO-LUMO, NBO, and molecular docking analysis of N-ethyl-N-nitrosourea, a potential anticancer agent. *Journal of Molecular Structure*, 1154, 39–50.

Ugwu, D. I., Okoro, U. C., Ukoha, P. O., Gupta, A., & Okafor, S. N. (2018). Novel anti-inflammatory and analgesic agents: synthesis, molecular docking and in vivo studies. *Journal of enzyme inhibition and medicinal chemistry*, 33(1), 405–415.

Waheed, A., Muhammad, S., Gilani, M. A., Adnan, M., & Aloui, Z. (2021). A Systematic and Comparative Analysis of Four Major Classes of DFT Functionals to Compute Linear and Nonlinear Optical Properties of Benchmark Molecules. *Journal of Computational Biophysics and Chemistry*, 20(05), 517–528. https://doi.org/10.1142/s2737416521500307